Received: 20 May 2020 | Revised: 28 June 2021 | Accepted: 30 June 2021

DOI: 10.1111/mmi.14780

RESEARCH ARTICLE

WILEY

Vibrio fischeri imports and assimilates sulfate during symbiosis with *Euprymna scolopes*

Nathan P. Wasilko[1] | Josue S. Ceron[1] | Emily R. Baker[1] | Andrew G. Cecere[1] | Michael S. Wollenberg[2] | Tim I. Miyashiro[1]

[1]Department of Biochemistry and Molecular Biology, Pennsylvania State University, University Park, PA, USA

[2]Department of Biology, Kalamazoo College, Kalamazoo, MI, USA

Correspondence
Tim I. Miyashiro, Department of Biochemistry and Molecular Biology, Pennsylvania State University, University Park, PA, USA.
Email tim14@psu.edu

Present address
Nathan P. Wasilko, Charles River Laboratories, Malvern, PA, USA

Funding information
National Institute of Diabetes and Digestive and Kidney Diseases, Grant/Award Number: T32 DK120509; National Institute of General Medical Sciences, Grant/Award Number: R01 GM129133

Abstract

Sulfur is in cellular components of bacteria and is, therefore, an element necessary for growth. However, mechanisms by which bacteria satisfy their sulfur needs within a host are poorly understood. *Vibrio fischeri* is a bacterial symbiont that colonizes, grows, and produces bioluminescence within the light organ of the Hawaiian bobtail squid, which provides an experimental platform for investigating sulfur acquisition in vivo. Like other γ-proteobacteria, *V. fischeri* fuels sulfur-dependent anabolic processes with intracellular cysteine. Within the light organ, the abundance of a Δ*cysK* mutant, which cannot synthesize cysteine through sulfate assimilation, is attenuated, suggesting sulfate import is necessary for *V. fischeri* to establish symbiosis. Genes encoding sulfate-import systems of other bacteria that assimilate sulfate were not identified in the *V. fischeri* genome. A transposon mutagenesis screen implicated YfbS as a sulfate importer. YfbS is necessary for growth on sulfate and in the marine environment. During symbiosis, a Δ*yfbS* mutant is attenuated and strongly expresses sulfate-assimilation genes, which is a phenotype associated with sulfur-starved cells. Together, these results suggest *V. fischeri* imports sulfate via YfbS within the squid light organ, which provides insight into the molecular mechanisms by which bacteria harvest sulfur in vivo.

KEYWORDS
host–microbe interactions, sulfate assimilation, symbiosis, transport, Vibrio

1 | INTRODUCTION

Sulfur is an element that is necessary for microbial life. For example, sulfur is found in proteins as the amino acids cysteine and methionine, in Fe-S clusters associated with respiration, and in several coenzymes (Lensmire & Hammer, 2018). Therefore, basic cellular processes demand that microbes have access to sulfur sources within their environments. Many bacteria grow on sulfate (Kredich, 2008), which is the form of sulfur that is commonly found in oxic environments on Earth. As reviewed extensively elsewhere (Kredich, 2008), bacteria assimilate sulfate by first importing it into the cytoplasm, where it is transferred to the monophosphate moiety of ATP by ATP sulfurylase (CysN-CysD) to produce adenosine 5′-phosphosulfate (APS). APS kinase (CysC) phosphorylates APS to 3′-phosphoadenosine 5′-phosphosulfate (PAPS), which permits the reduction in the sulfur atom first to sulfite by PAPS sulfotransferase (CysH) and then to sulfide by NADPH-sulfite reductase (CysI-CysJ). The sulfide is used by *O*-acetyl-serine (thiol)-lyase (CysK) to convert *O*-acetyl-serine (OAS) into cysteine and acetate. Free cysteine is significant for bacterial growth because it serves as the intracellular source of sulfur that fuels all sulfur-dependent anabolic processes.

Seawater contains 27.7 mM sulfate (Millero, 2014), which can be assimilated by various marine microbes. The Gram-negative bacterium *Vibrio fischeri* is an example of a marine microbe that can grow

by assimilating sulfate (Singh et al., 2015; Wasilko et al., 2019). Genes encoding homologs of CysD, CysN, CysH, CysJ, and CysK are necessary for growth of *V. fischeri* on sulfate (Singh et al., 2015; Wasilko et al., 2019), and CysC and CysI homologs are also encoded within the genome of *V. fischeri* (Wasilko et al., 2019). In addition, the LysR-type transcription factor CysB promotes expression of the genes involved in sulfate assimilation and is, therefore, necessary for survival in seawater (Wasilko et al., 2019).

The life cycle of many strains of *V. fischeri* alternates between a free-living stage and one in symbiosis with certain squid and fish (Stabb & Visick, 2013), during which *V. fischeri* cells emit bioluminescence that the host uses for specific nocturnal behaviors. Among animals known to harbor *V. fischeri* symbionts, the Hawaiian bobtail squid, *E. scolopes*, is the best characterized and thought to use bioluminescence for counterillumination to camouflage itself from predators at night (Jones & Nishiguchi, 2004). To establish symbiosis, *E. scolopes* juveniles initially acquire *V. fischeri* cells from the marine environment, which then grow into light-emitting populations within the epithelium-lined cavities, or crypts, of a specialized structure called the light organ (Montgomery & McFall-Ngai, 1993). Every day at dawn, squid expel up to 95% of their *V. fischeri* populations into the seawater and then promote growth of the residual bacteria during the day (Lee & Ruby, 1994). The current model for nutrient acquisition by *V. fischeri* within the light organ is that host-derived proteins are degraded into peptides and amino acids that promote symbiont growth (Graf & Ruby, 1998). In addition, chitin, which is a polymer of N-acetylglucosamine, and glycerophospholipids serve as carbon sources in vivo that fuel growth and bioluminescence production (Schwartzman et al., 2015; Wier et al., 2010).

In contrast to the central metabolic pathways that fuel *V. fischeri* growth within the light organ, our understanding of sulfur metabolism in vivo is still in its infancy. An undefined cysteine auxotroph was shown to achieve 5% normal abundance within the light organ (Graf & Ruby, 1998), which hinted at the importance of sulfur metabolism by the symbiont for symbiosis establishment. We recently reported that growth of *V. fischeri* within the light organ depends on the transcription factor CysB, suggesting that CysB-dependent transcription promotes symbiosis establishment (Wasilko et al., 2019). In addition, expression of an A227D variant of CysB in the Δ*cysB* mutant enabled utilization of cystine (two cysteine molecules sharing a thiol bond), but not sulfate, as a sole sulfur source. Because this strain could also colonize juvenile squid, we hypothesized that *V. fischeri* is exposed to an unknown host-derived compound that yields cystine. Here, we provide evidence that *V. fischeri* growth within the light organ crypts is facilitated by import of cystine and sulfate. Based on the results of a screen to identify mutants unable to assimilate sulfate, i.e., cysteine auxotrophs, we update the model of sulfate assimilation for *V. fischeri*. We also identify YfbS as a putative sulfate importer that functions within the marine environment and during symbiosis. Together, these findings suggest that *V. fischeri* acquires at least two sources of sulfur within the squid light organ, which provides insight into molecular adaptations that promote the growth of bacterial symbionts within a host environment.

2 | RESULTS

2.1 | *V. fischeri* assimilates sulfate and imports cystine within the squid light organ

In γ-proteobacteria, CysK (OAS (thiol)-lyase) converts OAS and sulfide into cysteine and acetate (Hulanicka et al., 1974). With 79% identity to the CysK protein of *Escherichia coli*, VF_1893 is predicted to be the CysK homolog in *V. fischeri* (Ruby et al., 2005). Consistent with previous reports (Singh et al., 2015; Wasilko et al., 2019), a *VF_1893*-knockout mutant (Δ*cysK*) did not grow in media containing sulfate as the sole sulfur source (Figure 1), suggesting CysK is necessary for *V. fischeri* to assimilate sulfate. Growth on sulfate was restored with the introduction of *cysK* and its native promoter in single copy into the genome of the Δ*cysK* mutant (Figure S1), demonstrating genetic complementation.

Previously, we reported that a mutant containing a transposon insertion in *cysK* exhibits slightly lower CFU levels within the host relative to a wild-type strain (twofold decrease in median) but this difference was deemed not statistically significant (Wasilko et al., 2019). We suspected that the sample size used in that study ($N = 10$ per group) was too low to detect the small effect. Therefore, using the Δ*cysK* mutant described above, we conducted squid colonization experiments with larger sample size ($N = 30$). After exposure to an inoculum containing the Δ*cysK* mutant, juvenile squid emitted bioluminescence but at levels lower than animals in the wild-type (WT) control group (Figure 2a). CFU levels of animals colonized by the Δ*cysK* mutant were also attenuated (Figure 2b), with a four-fold decrease in median relative to wild-type levels. In addition, exposure of squid to the Δ*cysK*-derived strain expressing *cysK in trans* resulted in bioluminescence and CFU levels that were elevated relative to animals colonized by the Δ*cysK* mutant (Figure S2). These observations suggest: (i) *V. fischeri* assimilates some sulfate within the light organ, and (ii) a sulfur source other than sulfate is present within the host.

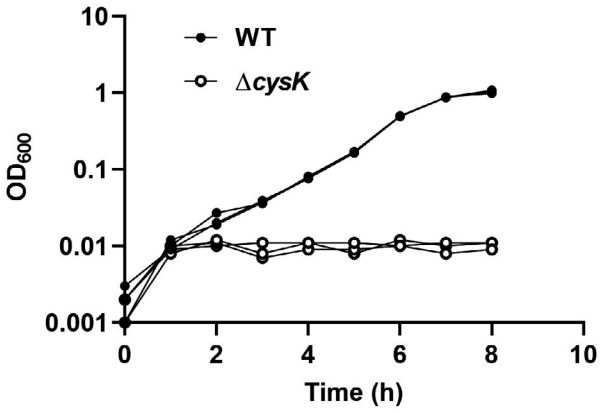

FIGURE 1 CysK promotes sulfate assimilation in *Vibrio fischeri*. Growth curves of ES114 (WT) and NPW90 (Δ*cysK*) in sulfate replete (50 mM sulfate) defined minimal medium. Each point represents a turbidity measurement (OD_{600}), and each curve represents an independent culture ($N = 3$). Experiment was performed two times with similar results obtained from both trials

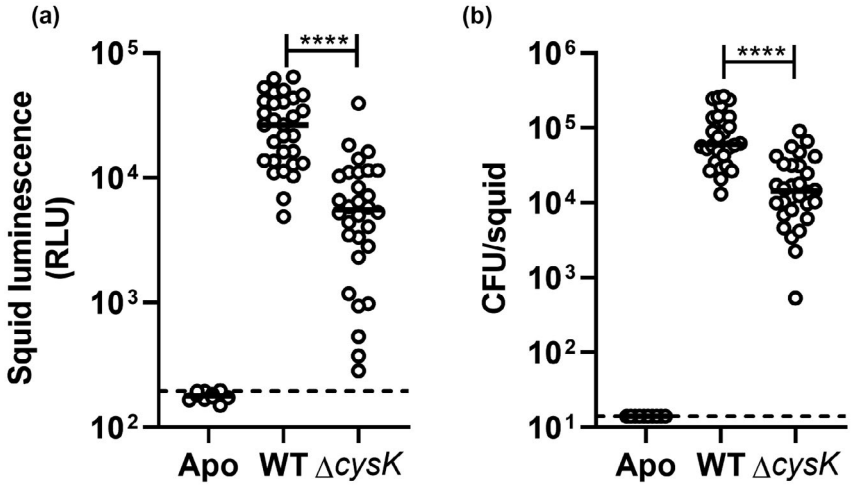

FIGURE 2 CysK is necessary for normal symbiosis establishment. (a). Luminescence emission by juvenile squid ($N = 30$) at 48 hr post-inoculation (p.i.), which was exposed to inoculums of ES114 (WT) or NPW90 (Δ*cysK*). Each point represents an individual animal, and each bar represents the median of the corresponding group. Dotted line represents the 95% percentile of luminescence measurements of animals ($N = 10$) exposed to a mock inoculum (Apo). Animals with luminescence emission levels above this line are deemed bioluminescent. RLU, relative light units. A two-tailed Mann–Whitney test was performed to test for statistical significance between group medians (****$p < .0001$). (b). Abundance of *Vibrio fischeri* in squid described in a. Each point represents an individual animal, and each bar represents the median of the corresponding group. Dotted line indicates limit of detection (14 CFU). A two-tailed Mann–Whitney test was performed to test for statistical significance between group medians (****$p < .0001$). Data shown in graphs are from one experimental trial. Experiment was performed twice using comparable N, and similar results were obtained from both trials

Our recent work suggests this sulfur source is related to cystine (Wasilko et al., 2019), which is comprised of two oxidized cysteine molecules linked by a disulfide bond. In fact, ectopic expression of the cystine importer TcyP in a Δ*cysB* mutant was sufficient to restore its ability to establish symbiosis (Figure S3). Thus, *V. fischeri* appears to be exposed to at least two sulfur sources within the light organ: sulfate and cystine.

Based on sulfur metabolism of enterics, sulfate and cystine are significantly different sulfur sources. Sulfate requires activation, phosphorylation, and reduction by eight electrons and the metabolite OAS to generate cysteine. In contrast, cystine requires reduction by only two electrons to yield two cysteine molecules, and this process bypasses the need for OAS. In enterics, a high intracellular level of OAS promotes the activity of the CysB transcription factor (Kredich, 1992). Therefore, to understand how *V. fischeri* responds to the sulfur sources available within the light organ, we determined the activity of the CysB transcription factor for host-associated populations. To monitor CysB-dependent transcriptional activation, we used a plasmid-based system containing *gfp* downstream of the promoter of *tcyJ* (P_{tcyJ}::*gfp*) (Figure 3a), which is regulated by CysB in *V. fischeri* (Figure S4) and predicted to encode a cystine-specific periplasmic binding protein associated with an ABC-type transporter (Chonoles Imlay et al., 2015). Activity of the *tcyJ* promoter (P_{tcyJ}) was lower in the crypts proximal to the light organ midline relative to other crypt types (Figure 3b), suggesting variation in CysB-dependent transcription between populations as previously reported for other CysB-activated genes (Wasilko et al., 2019). For the Δ*cysK* mutant, we observed lower levels of mCherry fluorescence relative to WT populations (Figure 3b), which is consistent with the lower abundance of CFUs recovered from the light organs colonized with this mutant (Figure 2b). In contrast, strong GFP fluorescence was detected in Δ*cysK* populations throughout the light organ (Figure 3b), suggesting high P_{tcyJ} activity. When averaged across the entire organ, P_{tcyJ} activity was 8.4-fold higher in Δ*cysK* populations relative to wild-type populations (Figure 3c), suggesting Δ*cysK* cells feature high CysB activity in vivo, presumably due to high intracellular OAS levels.

In *E. coli* and *Salmonella typhimurium*, OAS is synthesized by the serine acetyltransferase CysE, which is subject to feedback inhibition by intracellular cysteine (Kredich & Tomkins, 1966). Based on this model, we hypothesized that the high activity of CysB observed for Δ*cysK* populations in vivo (Figure 3) results from their intracellular cysteine levels being insufficient to inhibit CysE. When coupled with the observation of fewer Δ*cysK* CFU within the light organ (Figure 2b), this result suggests that Δ*cysK* cells become growth limited for sulfur in vivo. To test this hypothesis, we examined how the Δ*cysK* mutant responds to growth-limiting conditions of cystine. The Δ*cysK* mutant grew similar to wild-type cells unless the cystine levels were lower than 55 μM, which resulted in lower growth yields (Figure 4a). For lower concentrations of cystine (6.0 or 18.5 μM), we conclude that the cells grew until they had depleted the available cystine. To determine CysB activity under low cystine conditions, we used the P_{tcyJ}::*gfp* reporter to assess P_{tcyJ} activity in cells grown in 18.5 μM cystine. As wild-type cells grew, the level of P_{tcyJ} activity remained low until late stationary phase (Figure 4b), suggesting that CysB activity increased as environmental cystine was exhausted and sulfate became the only remaining sulfur source. The Δ*cysK* mutant, which could only utilize

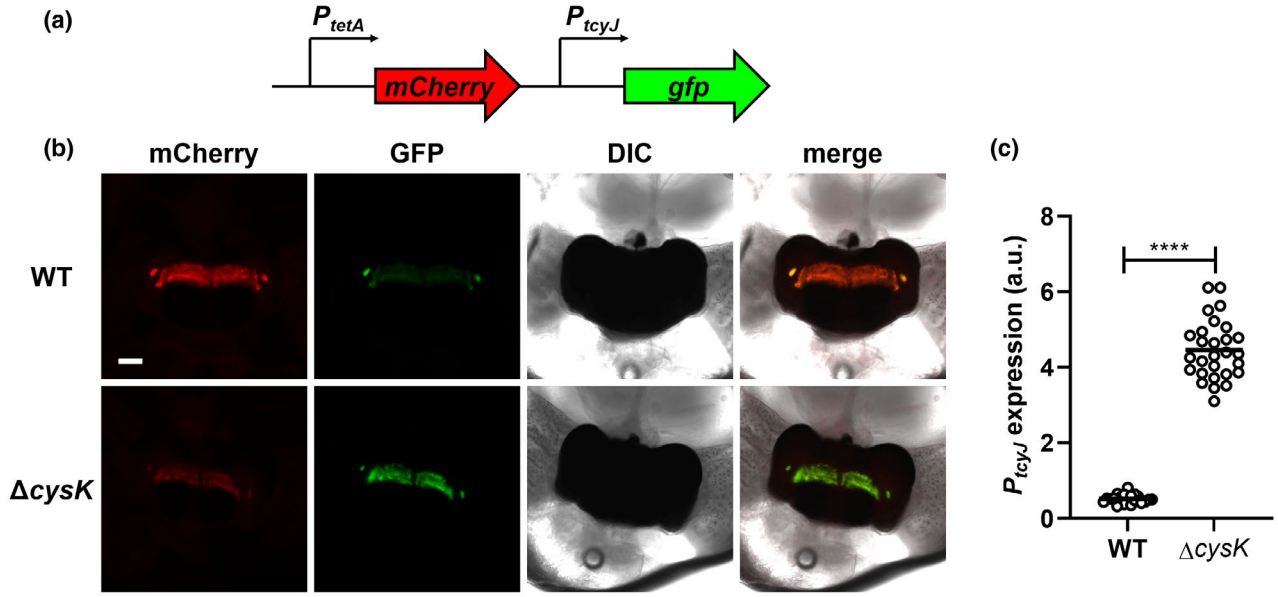

FIGURE 3 CysB-dependent transcription is elevated within host-associated cells that lack CysK. (a). GFP-based transcriptional reporter for P_{tcyJ} in plasmid pVF_0008P. Expression of mCherry depends on P_{tetA}. (b). Images of light organs colonized by ES114 (WT; top) or NPW90 (Δ*cysK*; bottom) harboring the P_{tcyJ} transcriptional reporter at 72 hr p.i. Scale bar =100 μm. (c). Quantification of P_{tcyJ} expression at 72 hr p.i. in light organs of squid colonized by ES114 (WT) or NPW90 (Δ*cysK*) harboring pVF_0008P (P_{tcyJ}::*gfp*). Each point represents P_{tcyJ} expression of host-associated *Vibrio fischeri* populations within an individual squid (WT: $N = 23$; Δ*cysK*: $N = 28$), and each bar represents the mean of the corresponding group. An unpaired, two-tailed *t* test with Welch's correction was performed to test for statistical significance between means (****p-value < .0001). Experiment was performed twice using comparable N, and similar results were obtained from both trials. Data shown in graph are from one experimental trial

the cystine, exhibited high P_{tcyJ} activity as the culture approached stationary phase (Figure 4b), suggesting OAS levels increased as the cystine was consumed. Thus, our results suggest that the host-derived sulfur source initially promotes growth of the Δ*cysK* mutant in vivo but becomes insufficient to maintain growth as the population expands. Consequently, we conclude that *V. fischeri* acquires the sulfur necessary to establish symbiosis by both assimilating sulfate and importing cystine within the host.

2.2 | Sulfate assimilation pathway in *V. fischeri*

Because sulfate assimilation is necessary for *V. fischeri* to survive in the marine environment and to grow within the light organ, we next sought to establish this pathway for *V. fischeri*. To accomplish this task, we applied the Basic Local Alignment Search Tool (BLAST) to the genome of *V. fischeri* strain ES114 using as queries the primary sequences of the factors in the sulfate assimilation pathway of *E. coli*. Homologs encoding the enzymes that activate sulfate (CysDN), reduce the sulfur atom (CysC, CysH, and CysIJ), and synthesize cysteine (CysK) are conserved in the *V. fischeri* genome (Table 1), with percent identities at the amino acid level ranging from 53% to 82%. CysE, which does not process any sulfur-containing substrate but instead synthesizes the precursor OAS, is also highly conserved. Finally, high conservation was also observed with CysB, which regulates transcription of all of the *cys* genes described above except *cysE* (Wasilko et al., 2019).

A different outcome arose with our search for homologs of the sulfate importers of *E. coli*. *E. coli* possesses two sulfate transport systems (Parra et al., 1983; Sirko et al., 1995): (i) an ABC-type transporter encoded by *cysUWA* that depends on the Sbp periplasmic binding protein for sulfate delivery, and (ii) a proton symporter encoded by *cysZ*. A homologue for Sbp was not identified in the genome of ES114 (Table 1), and the closest homologues for the CysUWA transporter exhibited low coverage, suggesting *V. fischeri* does not possess this transport system. In contrast, VF_1892 was identified as a potential homologue of CysZ. However, a mutant containing an in-frame deletion of *VF_1892* grew on sulfate (Figure S5), suggesting that there is at least one other sulfate transporter encoded by *V. fischeri*.

2.3 | *yfbS* encodes a transporter that facilitates sulfate assimilation

We next took a forward genetics approach to identify this alternative sulfate transporter. Mutants that fail to import sulfate cannot assimilate sulfate, that is, they would be unable to grow on sulfate as a sole sulfur source (so-called cysteine auxotrophs) (Kredich, 2008). LBS medium supports the growth of *V. fischeri* cysteine auxotrophs, such as the Δ*cysK* mutant (Figure 5a,b), presumably due to the presence of cysteine in the peptides that comprise this rich medium. After 24 hr of growth on solid LBS medium, activity of the *tcyJ* promoter was 5.3-fold higher in the Δ*cysK* mutant than in WT (Figure 5b,c),

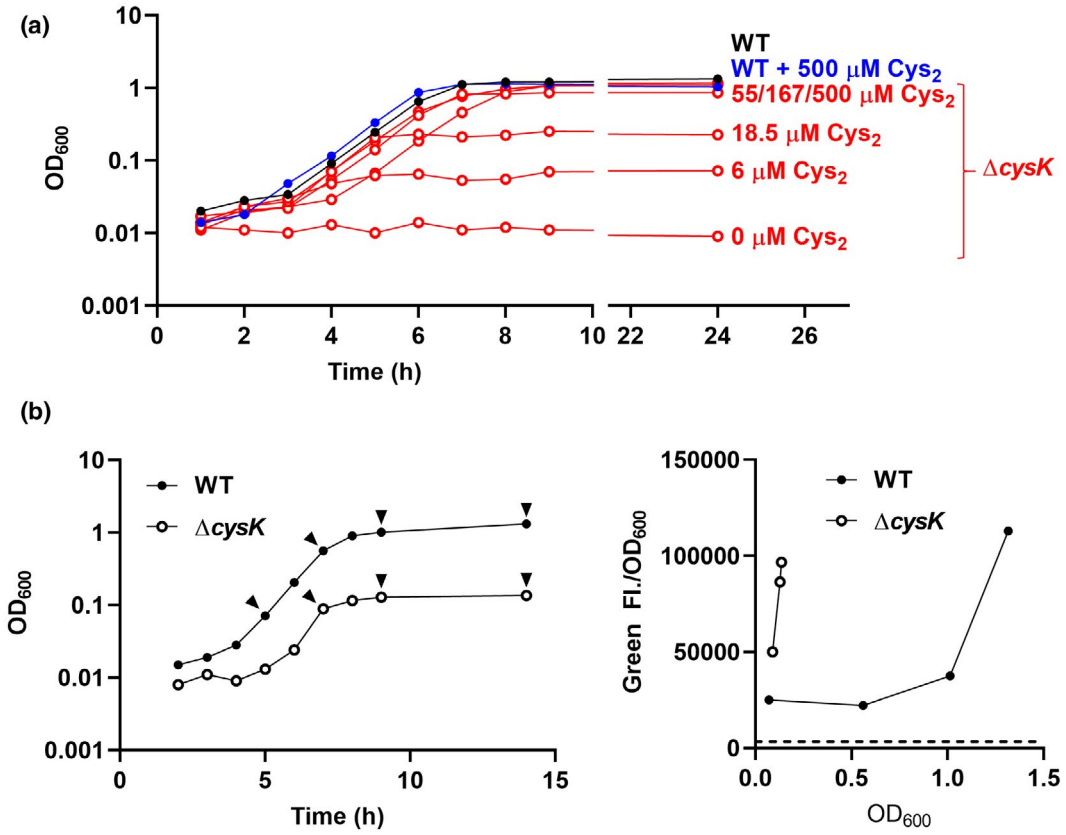

FIGURE 4 Cystine depletion promotes CysB-dependent transcription in cells that lack CysK. (a). Growth curves of ES114 (WT; closed symbols) and NPW90 (Δ*cysK*; red lines and open symbols) in sulfate replete defined minimal medium supplemented with the indicated amount of cystine (Cys_2). For WT curves, black and blue line indicate 0 and 500 μM Cys_2, respectively. Each curve represents a single culture that was sampled at the indicated times. Experiment was performed twice with similar results obtained from both trials. Data shown in graphs are from one experimental trial. (b). *Left*, growth curves of ES114 (WT; closed symbols) and NPW90 (Δ*cysK*; open symbols) harboring the P_{tcyJ} transcriptional reporter (pVF_0008P) in sulfate replete, defined minimal medium supplemented with 18.5 μM cystine. Each curve represents a single culture that was sampled at the indicated times. Arrowheads indicate samples examined for expression of P_{tcyJ}. *Right*, levels of green fluorescence normalized by OD_{600} for samples described in the left panel. Dotted line indicates auto-fluorescence associated with a non-fluorescent control strain. Experiment was performed twice with similar results obtained from both trials. Data shown in graph are from one experimental trial

which suggests that cysteine auxotrophs accumulate OAS as the peptide-derived sulfur sources within the medium are depleted. Therefore, as cysteine auxotrophs, strains unable to import sulfate should similarly exhibit elevated P_{tcyJ} activity when grown on LBS. To isolate cysteine auxotrophs of *V. fischeri*, we introduced by conjugation the P_{tcyJ}::*gfp* reporter plasmid into a Tn*5*-mutant library of ES114, selected for conjugants on LBS medium, and screened the resulting colonies for elevated GFP fluorescence. From screening ~10^5 CFU, 65 mutants with elevated P_{tcyJ} activity were isolated. We determined the transposon-insertion site within 29 of the mutants, which identified 9 genes (Table 2).

Genes that contained an insertion included *cysD*, *cysH*, *cysI*, *cysJ*, and *cysK* (Table 2), which are predicted to encode enzymes necessary for sulfate assimilation. Consistent with this model, representative transposon mutants for each gene failed to grow on sulfate as the sole sulfur source (Table 2). Transposon-insertion mutants for *cobA* and *VF_1531* also failed to grow on sulfate alone (Table 2), which is consistent with their predicted roles in the synthesis of the essential siroheme cofactor of CysIJ sulfite reductase (Crane & Getzoff, 1996). In *E. coli*, the *cysG* gene encodes siroheme synthase and its N- and C-termini exhibit significant identity with *cobA* and *VF_1531*, respectively (Table 1). The *yfcA* gene, which is predicted to encode an inner membrane protein, was also hit in the screen multiple times (Table 2), but the ability of the corresponding transposon mutants to grow on sulfate led to its exclusion from further evaluation in this study. The final gene identified from the screen was *yfbS*.

The *yfbS* gene is located within the *cysDN-yfbS-cysC* operon (Figure S6a), which genetically links *yfbS* to two enzymatic steps of assimilative sulfate reduction. YfbS is predicted to be a member of the solute carrier 13 (SLC13) family, which consists of sodium-coupled symporters that facilitate the transport of various ions, including sulfate, across the inner membrane (Pajor, 2006). YfbS is predicted to contain 12 transmembrane domains (TMDs), with two TrkA_C domains located within a large intracellular loop between TMDs 5 and 6 (Figure S6b). TrkA_C domains are predicted to bind ligands and are widespread in bacteria (Hoffmann et al., 2017). To

TABLE 1 *Vibrio fischeri* homologs of the proteins necessary for sulfate assimilation in *Escherichia coli*

E. coli		BLAST results		*V. fischeri*	
Protein	**Activity**	**Query cover**	**% Identity**	**Locus tag**	**Protein**
Sbp	Sulfate binding protein	No significant similarity found			
CysA	Sulfate/thiosulfate transport	67%	47.15%	VF_1315	PotA
		65%	46.86%	VF_A1091	AfuC
		96%	35%	VF_A0800	MalK
		77%	38.75%	VF_2149	VF_2149
CysW	Sulfate/thiosulfate transport	51%	29.8%	VF_1403	ModB2
		75%	23.71%	VF_2150	VF_2150
CysU	Sulfate/thiosulfate transport	73%	34.62%	VF_A0291	ModB2
		77%	28.5%	VF_1317	PotC
		76%	24.44%	VF_2150	VF_2150
CysP	Thiosulfate binding protein	9%	38.71%	VF_0805	VF_0805
CysD	ATP sulfurylase and catalytic subunit	100%	81.79%	VF_0320	CysD
CysN	ATP sulfurylase and GTP-binding unit	99%	63.92%	VF_0321	CysN
CysC	APS kinase	98%	65.15%	VF_0323	CysC
CysH	PAPS sulfotransferase	99%	69.96%	VF_0312	CysH
CysG	Siroheme synthase	54%	54%	VF_0773	CobA
		58%	33.46%	VF_1531	VF_1531
CysI	NADPH-sulfite reductase hemoprotein	97%	70.97%	VF_0311	CysI
CysJ	NADPH-sulfite reductase flavoprotein	98%	53.18%	VF_0310	CysJ
CysE	Serine transacetylase	97%	72.83%	VF_2347	CysE
CysM	O-Acetyl (thiol)-lyase-B	95%	44.48%	VF_1893	CysK
		98%	27.13%	VF_1579	VF_1579
CysK	O-Acetyl (thiol)-lyase-A	100%	78.64%	VF_1893	CysK
CysB	Transcription activator	99%	74.22%	VF_1490	CysB
CysZ	Sulfate transport	98%	62.9%	VF_1892	CysZ

Note: Escherichia coli proteins involved in sulfate assimilation were previously reported (Kredich, 2008). Query cover is the percentage of the query sequence (*E. coli* protein) that is covered by the target sequence (*Vibrio fischeri* protein) from performing BLAST. Percent identity is the percentage of amino acids that are identical between the query and target sequences within the covered query.

date, PerO of the alphaproteobacterium *Rhodobacter capsulatus* is the best characterized member of a SLC13 family member that contains TrkA_C domains, and it functions as a low-affinity oxyanion permease (Hoffmann et al., 2017). Among representative taxa of the 23 clades that comprise the *Vibrionaceae* family, a YfbS homolog was identified in 20 clades (Figure 6a). Furthermore, taxa encoding a YfbS homolog harbored the *yfbS* gene directly upstream of *cysC* (Table S1), which is the same gene synteny observed in *V. fischeri* (Figure S6a). Together, these findings show that YfbS is broadly conserved among *Vibrionaceae* and suggest that its function as a transporter is linked to assimilative sulfate reduction.

To investigate whether YfbS affects sulfate assimilation, we generated an in-frame deletion mutant of *yfbS* (Δ*yfbS*) and tested its ability to grow on sulfate. The Δ*yfbS* mutant did not grow on sulfate (Figure 6b), and expression of *yfbS in trans* (P_{trc}-*yfbS*) restored its ability to grow in this condition, demonstrating genetic complementation. We also tested whether ectopic expression of *yfbS* could promote growth on sulfate by a Δ*cysA* mutant of *E. coli*, which lacks the ATPase that facilitates sulfate import via the CysUWA transporter (Parra et al., 1983) and cannot grow on sulfate as a sole sulfur source (Figure 6c). Relative to the vector control, induction of *yfbS* expression enabled growth of the Δ*cysA* mutant on sulfate (Figures 6c and S7). We attribute the lower growth yield of these samples to some toxicity in *E. coli* from the expression of *yfbS* (Figures 6c and S8); however, extending the period of incubation enabled the Δ*cysA*-mutant expressing *yfbS* to achieve higher turbidity (Figure S9). Finally, we assessed whether YfbS promotes sulfate import in *V. fischeri* using a [^{35}S] sulfate-uptake assay. Both wild-type and Δ*yfbS* cells were initially grown in defined minimal medium supplemented with 0.1 mM sulfate and 18.5 μM cystine. Following exposure to [^{35}S] sulfate in the presence of cystine, wild-type cells showed increased radioactivity over time (Figure 6d), which suggests they imported sulfate. In contrast, the signal associated with the Δ*yfbS* mutant remained low (Figure 6d), which indicates poor sulfate uptake by the mutant and suggests YfbS is necessary for the import of sulfate. Taken together, these results

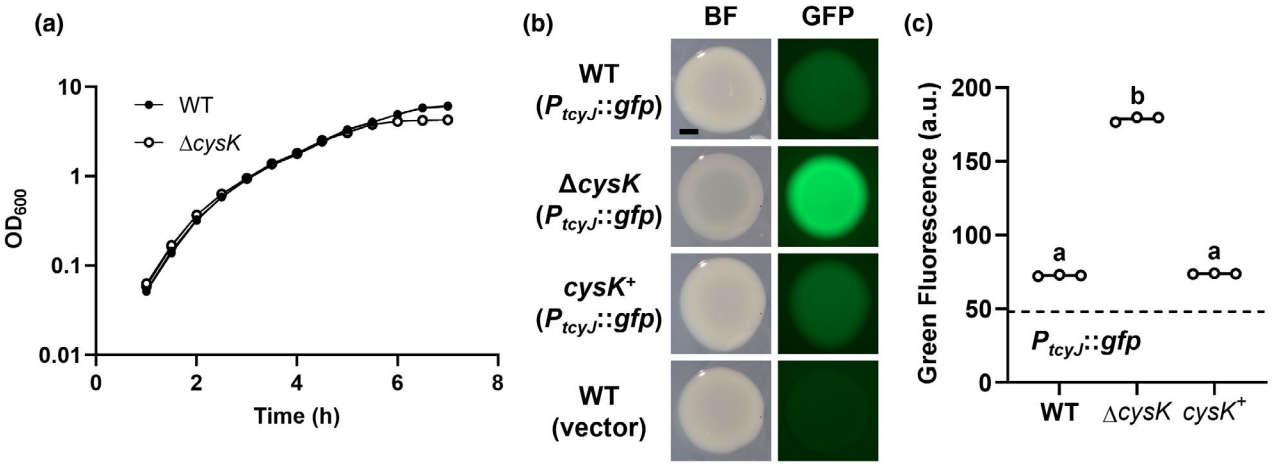

FIGURE 5 Growth of and CysB-dependent transcription in cysteine auxotrophs in rich medium. (a). Growth curves of ES114 (WT; closed symbols) and NPW90 (Δ*cysK*; open symbols) in LBS medium. Each curve represents an independent culture ($N = 3$). Differences between replicates is smaller than resolution allows. Experiment was performed twice with similar results obtained from both trials. (b). Images of spots of ES114 (WT), AGC10 (Δ*cysK*), or AGC09 (*cysK*$^+$) harboring pVF_0008P (P_{tcyJ}::*gfp*) or pVSV105 (vector) grown on LBS for 24 hr. Scale bar = 1 mm. (c). Quantification of P_{tcyJ} expression in strains harboring pVF_0008P grown as described in panel B. Each point represents the green fluorescence of an individual spot, and bars represent the group means. Dotted line indicates mean auto-fluorescence associated with spots of the non-fluorescent vector control pVSV105/ES114 ($N = 3$). A one-way ANOVA test demonstrated statistical significance between group means ($F_{2,6} = 9{,}407$, p-value < .0001). A Tukey's *post hoc* test was performed to statistically compare the means of each group, with different letters indicating p-value < .0001 and same letters indicating p-value > .05, with p-values adjusted for multiple comparisons. Experiment was performed twice with similar results obtained from both trials

TABLE 2 Genes identified from screen for Tn*5* insertion mutants with increased P_{tcyJ} activity

Locus tag	Gene	Putative function	#Unique insertions	[a]Growth on SO_4^{2-}
VF_0310	*cysJ*	Sulfite reductase subunit alpha	1	–
VF_0311	*cysI*	Sulfite reductase	1	–
VF_0312	*cysH*	PAPS reductase A subunit	3	–
VF_0320	*cysD*	Sulfate adenylyltransferase	1	–
VF_0322	*yfbS*	Divalent anion: sodium symporter family protein	2	–
VF_0773	*cobA*	Urophorphyrin-III C-methyltransferase	3	–
VF_1008	*yfcA*	Inner membrane protein	8	+
VF_1531	*VF_1531*	Ferrochelatase	3	–
VF_1893	*cysK*	*O*-Acetyl (thiol)-lyase A	3	–

[a]Mutants were assessed for ability to form colonies on sulfate-replete DMM, (–) = no growth, and (+) = growth.

suggest YfbS is the transporter supporting sulfate assimilation in *V. fischeri*.

2.4 | YfbS promotes sulfate assimilation within the squid light organ

To complete this study, we investigated the impact of YfbS on symbiosis. Because part of the life cycle of symbiotic *V. fischeri* strains includes a free-living stage in the marine environment (Lee & Ruby, 1994), we first examined the viability of Δ*yfbS* mutant in seawater, which contains 27.7 mM sulfate (Millero, 2014). CFU levels of the Δ*yfbS* mutant decreased over time (Figure 7a), presumably due to cells failing to replenish intracellular cysteine via sulfate assimilation. We next conducted squid colonization experiments by exposing juvenile squid to an inoculum containing the Δ*yfbS* mutant. Relative to the WT control group, squid exposed to the Δ*yfbS* mutant exhibited lower bioluminescence (2.6-fold lower median) and attenuated CFU levels (3.6-fold lower median) (Figure 7b), suggesting that sulfate import promotes the ability of *V. fischeri* to establish symbiosis. Finally, to gain insight into the cellular physiology of Δ*yfbS* cells in vivo, we examined CysB-dependent transcription within host-associated populations of the mutant. We observed elevated P_{tcyJ} activity (Figure 7c,d), suggesting that the Δ*yfbS* cells have high OAS levels in vivo. Together, these data suggest that host-associated populations of

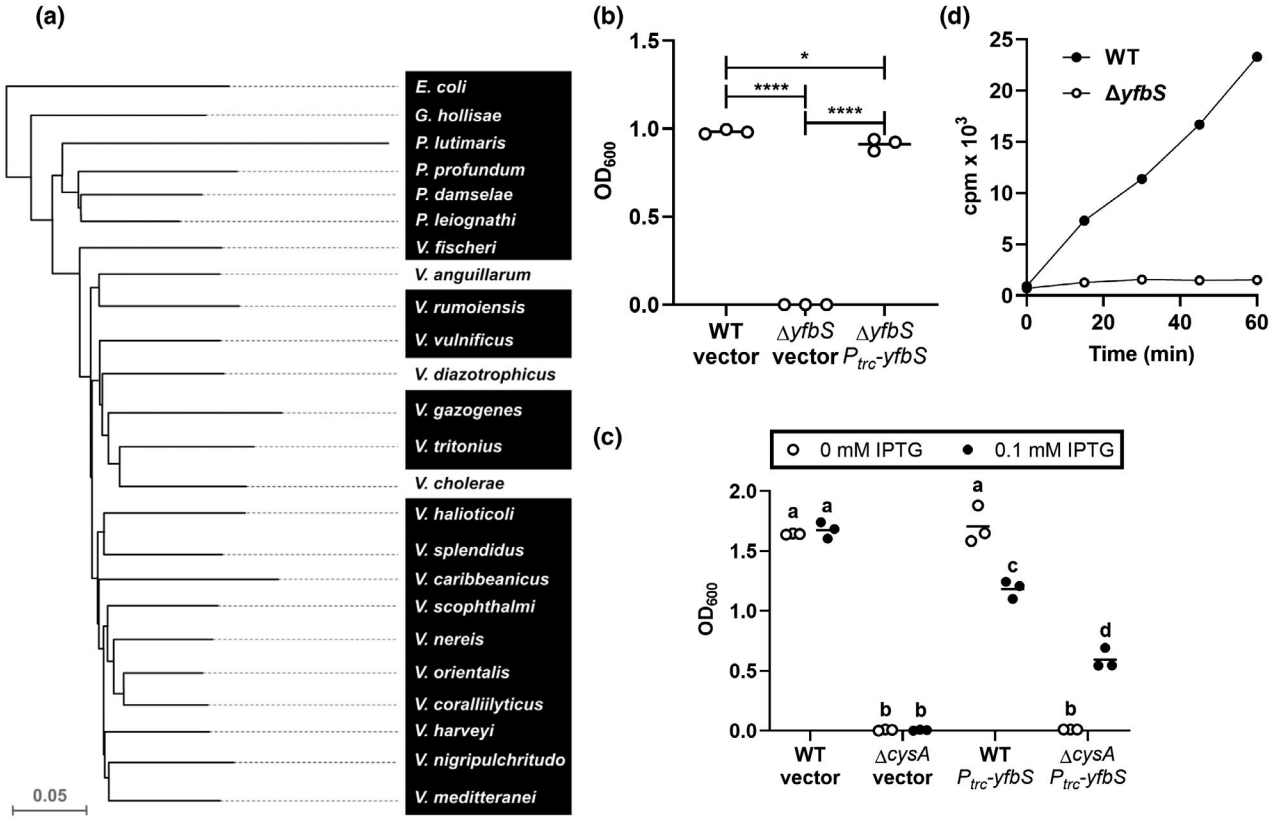

FIGURE 6 *yfbS* encodes a conserved transporter that promotes sulfate assimilation in *Vibrio fischeri*. (a). Phylogenetic tree for taxa that represent the major clades of *Vibrionaceae*. Tree is based on the multi-gene supertree reported previously (Sawabe et al., 2013). All taxa listed encode a CysC homolog. Taxa highlighted in black encode a YfbS homolog. Locus tags of CysC and YfbS homologs are listed in Table S1. (b). Turbidity of cultures of ES114 (WT) and NPW88 (Δ*yfbS*) harboring either pTM214 (vector) or pNW032 (P_{trc}-*yfbS*) after 21 hr of incubation in sulfate-replete DMM supplemented with 1 mM IPTG. Each point represents the optical density (OD_{600}) of an individual culture ($N = 3$). A one-way ANOVA revealed statistically significant differences between means ($F_{2,6} = 2011$, p-value < .0001). A Tukey's *post hoc* test was performed to statistically compare the means of each group, with p-values adjusted for multiple comparisons (*$p < .05$, ****$p < .0001$). Experiment was performed twice with similar results obtained from both trials. (c). Turbidity of cultures of *Escherichia coli* strains BW25113 (WT) and JW2415 (Δ*cysA*) harboring either pTrc99a (vector) or pNW039 (P_{trc}-*yfbS*) after 21 hr of incubation in minimal A glucose medium ± 100 μM IPTG. Each point represents the optical density (OD_{600}) of an individual culture ($N = 3$). A two-way ANOVA test revealed statistically significant differences for genotype ($F_{3,16} = 773$, p-value < .0001) and interactions between genotype and IPTG treatment ($F_{3,16} = 58.37$, p-value < .0001), but not IPTG treatment alone ($F_{1,16} = 0.6470$, p-value = .433). A Tukey's *post hoc* test was performed to statistically compare the means of each group, with p values adjusted for multiple comparisons. Comparisons between groups labeled with different letters indicate statistical significance between their means (p-value < .0001) and those with the same letters not significant (p-value > .05). (d). Sulfate uptake by cultures of ES114 (WT) and NPW88 (Δ*yfbS*) that were grown in defined minimal medium supplemented with 0.1 mM sulfate and 18.5 μM cystine. At an OD_{600} of 0.8, cells were harvested and exposed to an [^{35}S] sulfate cocktail. Radioactivity of approximately 9.0×10^8 CFU was measured at the indicated time points. cpm, counts per minute. Experiment was repeated three times with similar results obtained from each trial

Δ*yfbS* are starved for sulfur, implying that YfbS imports sulfate within the squid light organ.

3 | DISCUSSION

Bacterial symbionts must acquire sulfur within their host to grow and contribute to the symbiosis, yet our understanding of the molecular mechanisms underlying sulfur import is still rudimentary for most symbionts. In this study, the squid–vibrio symbiosis provided a platform to investigate the mechanisms of sulfur acquisition by a bacterial symbiont within the host. In particular, we found that *V. fischeri* assimilates sulfate within the light organ (Figure 2), which supplements the sulfur source related to cystine that is provided by the host. As illustrated in Figure 8, we have updated the sulfate assimilation pathway for *V. fischeri* to include sulfate import and the synthesis of siroheme, which is an essential cofactor for sulfite reductase (Siegel et al., 1982). Sulfate import represents a key difference in the sulfate assimilation pathway between *V. fischeri* and other model organisms, for example, *E. coli*. Our results from bioinformatics and genetic experiments implicate the putative permease YfbS as the importer of sulfate for *V. fischeri* (Table 2 and Figure 6). We show that YfbS functions both in the marine environment and within the squid light organ (Figure 7).

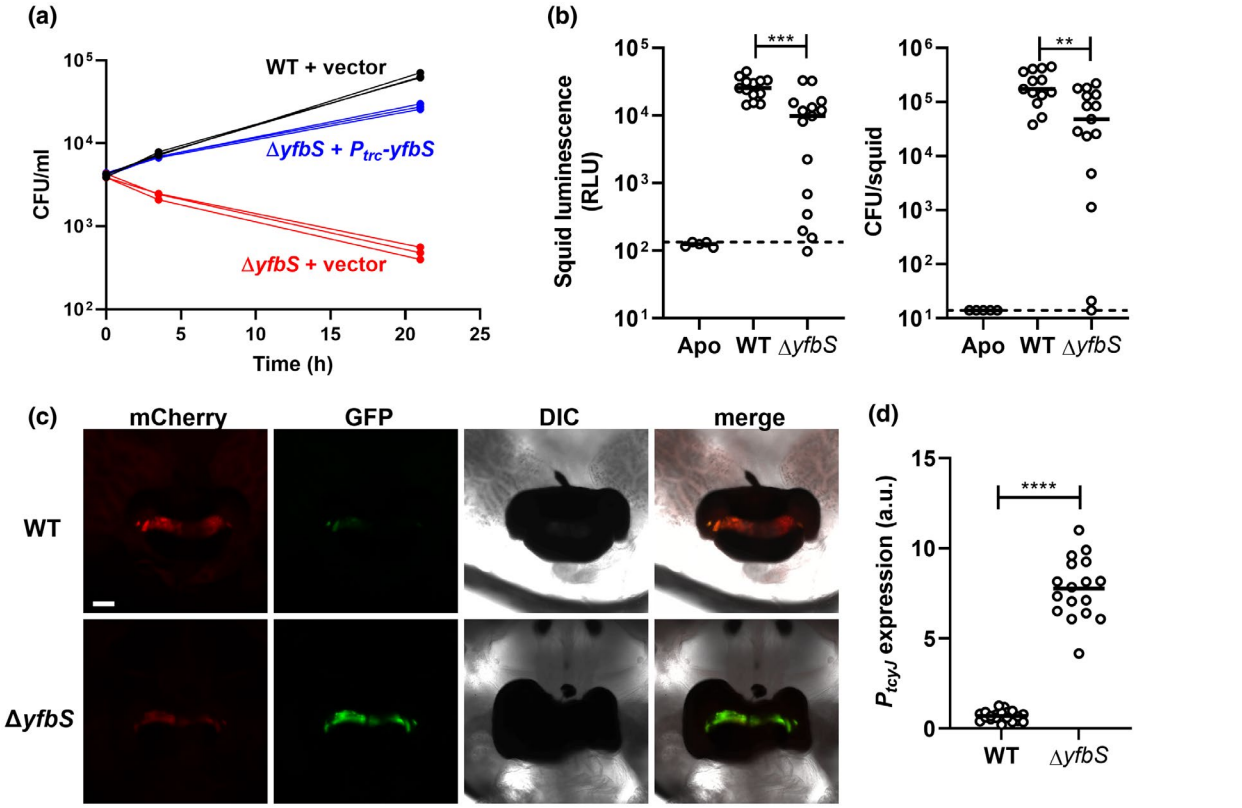

FIGURE 7 YfbS promotes sulfate assimilation during symbiosis establishment. (a). Abundance of ES114 (WT) or NPW88 (Δ*yfbS*) harboring pTM214 (vector) or pNW032 (P_{trc}-*yfbS*) in FSSW supplemented with 1 mM IPTG. Each point represents the concentration of recovered CFU (CFU/ml), and each line connecting points indicates an individual culture ($N = 3$). (b). *Left*, luminescence emission by juvenile squid ($N = 13–15$) at 48 hr p.i., which were exposed to inoculums of ES114 (WT) or NPW88 (Δ*yfbS*). Each point represents an individual animal, and each bar represents the median of the corresponding group. Dotted line represents the 95% percentile of luminescence measurements of animals ($N = 5$) exposed to a mock inoculum (Apo). Animals with luminescence emission levels above this line are deemed bioluminescent. RLU, relative light units. A two-tailed Mann–Whitney test was performed to test for statistical significance between group medians (***$p < .001$). *Right*, abundance of *Vibrio fischeri* in squid is shown in left. Each point represents an individual animal, and each bar represents the median of the corresponding group. Dotted line indicates limit of detection (14 CFU). A two-tailed Mann–Whitney test was performed to test for statistical significance between group medians (**$p < .01$). Data shown in graphs are from one experimental trial. Experiment was performed twice using comparable N, and similar results were obtained from both trials. (c). Images of light organs colonized by ES114 (WT; top) or NPW88 (Δ*yfbS*; bottom) harboring the P_{tcyJ} transcriptional reporter at 72 hr p.i. Scale bar = 100 μm. (d). Quantification of P_{tcyJ} activity at 72 hr p.i. in light organs of squid colonized by ES114 (WT) or NPW88 (Δ*yfbS*) harboring pVF_0008P (P_{tcyJ}::*gfp*). Each point represents an individual squid (WT: $N = 20$; Δ*yfbS*: $N = 28$), and each bar represents the median of the corresponding group. Image analysis described in methods. An unpaired, two-tailed *t* test with Welch's correction was performed to test for statistical significance between means (****p-value $< .0001$). Data shown in graph are from one experimental trial. Experiment was performed twice using comparable N, and similar results were obtained from both trials

From these findings, we propose a model for sulfur acquisition by *V. fischeri* (Figure 9). During the free-living stage of its life cycle, *V. fischeri* takes up inorganic sulfate via YfbS from the marine environment. With sulfate as the only sulfur source available for replenishing the intracellular pool of cysteine, the feedback inhibition on CysE is released, resulting in OAS synthesis. Consequently, CysB activates transcription of genes involved in sulfate assimilation, including the *cysDN-yfbS-cysC* operon. Upon colonizing the squid light organ, *V. fischeri* has access to cystine, presumably through auto-oxidation of cysteine that is released from degradation of host proteins (indicated by the dotted arrow in Figure 9). Cystine can be imported by at least three transport systems: TcyP, TcyJLN, and an unknown transporter. However, it appears that the import of cystine by these transporter systems and sulfate by YfbS are both necessary to meet the sulfur demands of *V. fischeri* for rapid growth and bioluminescence production in vivo; the latter of which could be equivalent to at least 10% of cellular energy (ATP turnover) (Bose et al., 2008). Because small molecules can still be exchanged between the crypt spaces and exterior environment through the ducts, we hypothesize that the primary source of sulfate remains seawater. However, the import of cystine, which contributes to intracellular cysteine pools, results in lowered CysB-dependent transcription, suggesting that cells conserve some energy by decreasing their dependence on sulfate assimilation.

YfbS is a member of the ArsB/NhaD ion transporter superfamily, with similarity to the PerO-like permeases that feature TrkA_C domains. PerO was first described as the low-affinity molybdate

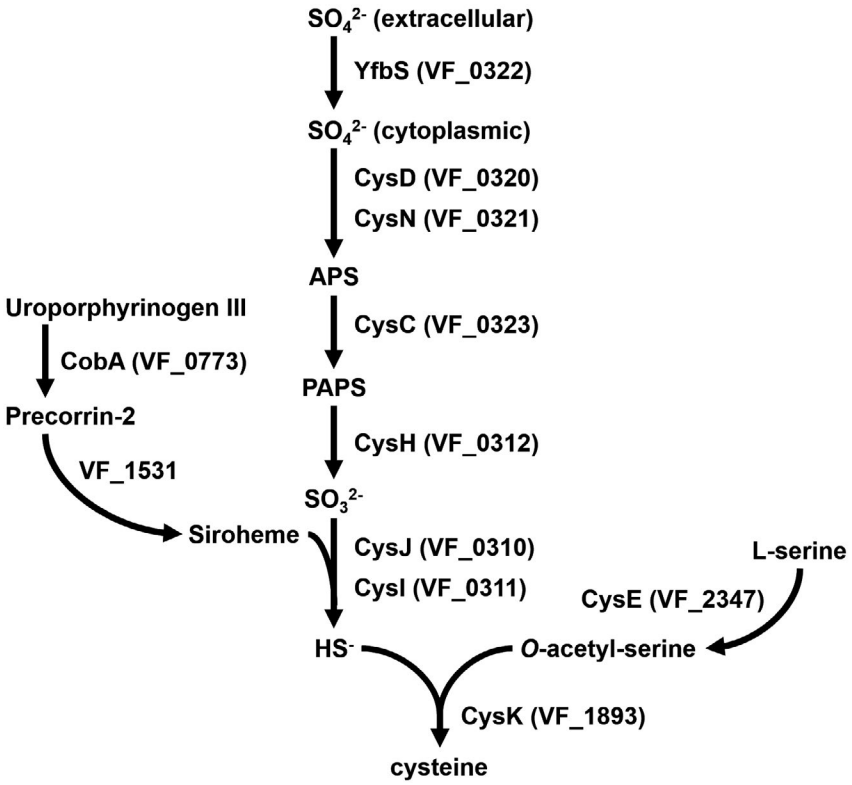

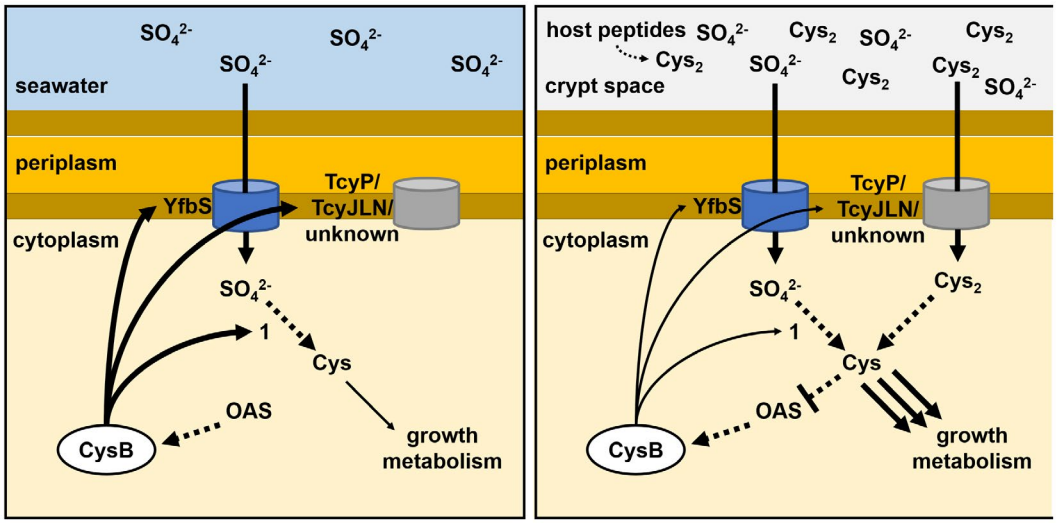

FIGURE 8 Model of sulfate assimilation in *Vibrio fischeri*. This model represents an updated version of one presented previously (Wasilko et al., 2019). Nodes indicate intermediate sulfur compounds, cofactors, and other substrates involved in sulfate assimilation. Arrows are labeled with the genetic factors encoded by *V. fischeri* that facilitate each step. APS, adenosine-5′ phosphosulfate; OAS, O-acetyl-serine; PAPS, 3′-phosphoadenosine-5′-phosphosulfate

FIGURE 9 Model of CysB-dependent sulfur import in *Vibrio fischeri*. *Left*, within the marine environment, sulfate is the primary sulfur source and imported into *V. fischeri* via YfbS. The sulfate is assimilated by synthesizing cysteine (1), which promotes viability and growth in seawater. High *O*-acetyl-serine (OAS) levels promote CysB-dependent expression of factors involved in sulfate assimilation, sulfate import (YfbS), and cystine importers (e.g., TcyP). *Right*, in the light organ, *V. fischeri* growth is accelerated due by accessing host-derived peptides, which are presumed to serve as a source of cysteine that auto-oxidizes to cystine. To meet the demand for sulfur, cells supplement sulfate assimilation by importing cystine, which boost cysteine pools. This increased flux of cysteine leads to lower OAS levels through feedback inhibition over CysE, which in turn decreases CysB-dependent transcription

permease in the phototrophic alphabacterium *R. capsulatus* (Gisin et al., 2010), which incorporates molybdenum (Mo) into several enzymes, including a Mo-dependent nitrogenase. In addition to PerO, *R. capsulatus* imports molybdate with the high-affinity ModABC (ABC-type) transporter. Molybdate is cytotoxic at high concentrations due to its ability to substitute for sulfate as a substrate for ATP sulfurylase, leading to a futile cycle that simply cleaves ATP to adenylic acid and pyrophosphate (Gisin et al., 2010). Consequently, under high Mo concentrations, *R. capsulatus* lowers molybdate import by decreasing *modABC* expression (Kutsche et al., 1996). However, PerO expression is independent of molybdate concentration (Gisin et al., 2010), suggesting that the cellular requirements

for Mo are achieved through the constitutive expression of PerO with supplementation by induction of ModABC as needed. Due to the presence of *yfbS* within the same operon as several *cys* genes, *V. fischeri* appears to regulate the titer of the sulfate permease by CysB and, thus, in conjunction with sulfate assimilation. Interestingly, in addition to molybdate, PerO also transports sulfate, tungstate, and vanadate into *R. capsulatus*, suggesting the permease may provide versatility as a general oxyanion importer. Future work examining the specificity of YfbS will determine whether *V. fischeri* can import other oxyanions via this permease.

In addition to the PerO-like permease, sulfate transporters from four other families (SulT, SulP, CysP, and CysZ) have been identified in bacteria (Aguilar-Barajas et al., 2011). *E. coli*, which served as the reference organism for sulfate assimilation in this study, possesses SulT (CysUWA) and CysZ transport systems (Kredich, 2008). CysZ is an integral membrane protein with a hexameric structure that facilitates sulfate translocation (Assur Sanghai et al., 2018). While *V. fischeri* encodes a homologue of CysZ, no growth defect was observed for the Δ*cysZ* mutant in media containing sulfate as a sole sulfur source (Figure S5), precluding our ability to test its impact on sulfur metabolism in *V. fischeri*. The SulT transport system of *E. coli* is the ABC-type transporter that depends on the periplasmic binding protein Sbp for delivery of the oxyanion to the transporter. The K_m of the homologous CysUWA-Sbp transporter of *S. typhimurium* in whole cells for sulfate is 36.8 μM (Dreyfuss, 1964), and the affinity of Sbp for sulfate is 0.1 μM (Pardee, 1966), suggesting that this system acts as a high-affinity sulfate transporter. With sulfate prevalent in the marine environment at 27.7 mM, a high-affinity transporter such as the one expressed by *S. typhimurium* and *E. coli* is unnecessary for *V. fischeri*. Thus, importing sulfate via a permease from a sulfate-replete environment represents a solution for *V. fischeri* to consume less energy equivalents than an ABC-type transport system. The prevalence of YfbS homologs throughout many taxa of *Vibrionaceae* (Figure 6a) suggests that this transporter is a major mechanism for importing sulfate by members of this important family of bacteria. Additionally, the absence of a *yfbS* gene in subclades containing *Vibrio cholerae O1 biovar El Tor*, *Vibrio anguillarum*, and *Vibrio diazotrophicus* (Figure 6a) represents an opportunity to gain insight into ecological diversity of the *Vibrionaceae* family by exploring alternative sulfur-acquisition mechanisms among these taxa.

Our report represents part of an expanding body of literature that highlights the importance of sulfur acquisition and its regulation for bacterial growth within a host. For example, the human pathogen *Staphylococcus aureus* scavenges cystine within heart and liver infections (Lensmire et al., 2020). To import cystine, *S. aureus* expresses TcyP symporter and TcyABC, with either necessary for normal fitness during heart infections but only TcyP contributing to fitness within liver infections. Transcription of both transport systems is under negative regulation by the CymR repressor, which responds to OAS by releasing DNA (Soutourina et al., 2009). Thus, for *S. aureus*, optimal fitness may depend on each transporter being expressed to a level that is specific to each tissue type. Recent work with *Serratia marcescens* has revealed 1,130 genes exhibit at least a twofold change between sulfate-replete and sulfate-limited growth conditions (Anderson et al., 2019). Sulfate is a normal constituent of serum and urine (Psychogios et al., 2011; Wishart et al., 2018), which offers a source of sulfur for bacteria within these habitats. Genes encoding phospholipase and hemolysin, which are known virulence factors of *S. marcescens*, were upregulated in the presence of sulfate (Anderson et al., 2019). Therefore, sulfate assimilation by *S. marcescens* appears to serve as a cue for this pathogen to express its virulence factors within a host. The findings we present here broaden the significance of investigating sulfur metabolism in host–microbe interactions by demonstrating its impact on the ability of a bacterial symbiont to establish symbiosis with its natural host.

At this time, the source of cystine within the host remains unknown and is, therefore, an exciting direction to investigate. Proteolysis has the potential to release peptides containing cysteine residues that have been detected in the exudate (Graf & Ruby, 1998), which may also serve as alternative sulfur sources. Thus, approaches based on imaging mass spectrometry, which has the capability to locate specific compounds within juvenile squid (Zink et al., 2020), will be invaluable in further refining the model presented here.

In summary, it is now apparent that *V. fischeri* utilizes multiple transporters to import at least two sulfur sources within the host. Many questions remain, including how *V. fischeri* acclimates to the host-derived sulfur source during initial colonization of the light organ. This finding provides a platform for future research endeavors centered on sulfur metabolism that will determine the molecular adaptations that enable bacterial symbionts to grow and function within a host environment.

4 | MATERIALS AND METHODS

4.1 | Media and growth conditions

V. fischeri strains were grown aerobically at 28°C in LBS medium or defined minimal medium (DMM) containing 10 mM N-acetylglucosamine as described previously (Wasilko et al., 2019). To maintain plasmids during growth in culture, chloramphenicol was used at 2.5 μg/ml. Cysteine auxotrophs were propagated on medium supplemented with 1 mM cysteine. *E. coli* strains were grown aerobically at 37°C in LB medium (1% [wt/vol] tryptone, 0.5% [wt/vol] yeast extract, and 1% [wt/vol] NaCl) or minimal A medium (Miller, 1972) supplemented with 0.2% glucose and 1 mM $MgSO_4$.

To initiate cultures of *V. fischeri* in DMM, starter cultures grown in LBS overnight were first normalized to an OD_{600} = 1.0 and then diluted 1:100 into LBS medium. Upon reaching OD_{600} = 1.0, cells were concentrated by centrifugation at 5,000×*g* and washed in DMM twice, and then, diluted into DMM. To initiate cultures of *E. coli* in minimal A medium, starter cultures grown in LB overnight were first normalized to an OD_{600} = 1.0 and then diluted 1:100 into LB medium. Upon reaching OD_{600} = 0.5, cells were concentrated by centrifugation at 5,000×*g* and washed in minimal A medium twice and then diluted into DMM.

4.2 | Strains and plasmids

All strains and plasmids used in this study are listed in Table 3. Primers used in their construction are listed in Table 4.

4.2.1 | Construction of deletion alleles

The deletion alleles for Δ*cysZ* (NPW87), Δ*yfbS* (NPW88), and Δ*cysK* (NPW90) were constructed using PCR splicing by overlap extension and natural transformation, as described elsewhere (Guckes et al., 2020; Visick et al., 2018).

TABLE 3 Strains and plasmids used in this study

Strain	Genotype	References
ES114	Wild-type *V. fischeri*	Ruby et al. (2005)
NPW03	ES114 Δ*cysB*	Wasilko et al. (2019)
NPW87	ES114 Δ*cysZ*	This study
NPW88	ES114 Δ*yfbS*	This study
NPW90	ES114 Δ*cysK*	This study
TIM313	ES114 Tn*7*::[*erm*]	Wasilko et al. (2019)
TIM409	ES114 Δ*cysB* Tn*7*::[*cysB erm*]	Wasilko et al. (2019)
TIM410	ES114 Δ*cysB* Tn*7*::[*erm*]	Wasilko et al., (2019)
TIM411	ES114 Δ*cysB* Tn*7*::[*cysB*A227D *erm*]	Wasilko et al. (2019)
AGC09	ES114 Δ*cysK* Tn*7*::[*cysK erm*]	This study
AGC10	ES114 Δ*cysK* Tn*7*::[*erm*]	This study
BW25113	Δ*(araD-araB)567*, Δ*lacZ4787*(::rrnB-3), λ-, *rph-1*, Δ*(rhaD-rhaB)568*, and *hsdR514*	Datsenko and Wanner (2000)
JW2415	BW25113 Δ*cysA751*::*kan*	Baba et al. (2006)
JW2406	BW25113 Δ*cysZ742*::*kan*	Baba et al. (2006)
pEVS79	pBC SK(+) *oriT cat*	Stabb and Ruby (2002)
pEVS104	R6Kori RP4 *oriT trb tra kan*	Stabb and Ruby (2002)
pEVS107	R6Kori RP4 *oriT mini*-Tn*7 mob erm kan*	McCann et al. (2003)
pVF_0008P	pTM267 Δ*kan* P_{tcyJ}-*gfp*	This study
pVSV105	R6ori *ori*(pES213) RP4 *oriT cat*	Dunn et al. (2006)
pTM214	pVSV105 *lacI*^{q} P_{trc}::*mCherry*	Miyashiro et al. (2011)
pTM267	pVSV105 P_{tetA}-*mCherry kan*::*gfp*	Miyashiro et al. (2010)
pTrc99A	*lacI*^{q} P_{trc}-MCS *bla*	Amann et al. (1988)
pSCV51	pTM267 P_{proD}::*gfp*	This study
pNW030	pTM267 P_{proD}::*tcyP*	This study
pNW032	pVSV105 *lacI*^{q} P_{trc}-*yfbS*	This study
pNW039	pTrc99A (P_{trc}-*yfbS*)	This study
pAC03	pEVS107 *cysK*	This study
pKV494	pJET +FRT-Em^r	Visick et al. (2018)
pKV496	pEVS79-Kn^r +flp$^+$	Visick et al. (2018)
pUX-BF13	R6Kori *tns bla*	Bao et al. (1991)

4.2.2 | Construction of P_{tcyJ}::*gfp* reporter plasmid

Plasmid pVF_0008P was constructed by amplifying the *tcyJ* promoter from ES114 genomic DNA and cloning the product into pCR blunt (Life Technologies, Carlsbad, CA, USA). After the insert was confirmed by sequencing, it was subcloned into pTM267 upstream of *gfp* via XmaI/XbaI restriction digests.

4.2.3 | Construction of *yfbS* overexpression vectors

Plasmid pNW032 was constructed by amplifying *yfbS* from ES114 genomic DNA and cloning the product into pCR blunt. Following sequencing to confirm the insert, the *yfbS* gene was subcloned downstream of the P_{trc} promoter in pTM214 via XmaI/SalI. Plasmid pNW039 was constructed by digesting pNW032 with SalI/MluI and subcloning the fragment containing *yfbS* into the SalI/MluI vector fragment of pTrc99A.

4.2.4 | Construction of *tcyP* overexpression vector

Plasmid pSCV51 was constructed by amplifying the synthetic promoter *proD* from a pSB3C5-derived plasmid and cloning into pCR blunt. The insert was confirmed by sequencing and subcloned into pTM267 via XmaI/XbaI. Plasmid pNW030 was generated by amplifying *tcyP* from ES114 genomic DNA and subcloning into pSCV51 via XmaI/XhoI.

4.2.5 | Construction of *cysK* complementation vector

Plasmid pAC03 was constructed by amplifying the *cysK* gene from ES114 genomic DNA and cloning the product into pCR blunt. The insert was confirmed by sequencing and subcloned into pEVS107 via KpnI/SpeI. Strains AGC10 and AGC09 were generated by integrating pEVS107 and pAC03, respectively, into Δ*cysK*-mutant NPW90 via pEVS104 and pUX-BF13, as previously described (Miyashiro et al., 2011).

4.3 | Squid colonization assays

Squid colonization assays were performed with slight modifications as previously described (Wasilko et al., 2019). Briefly, starter cultures grown in LBS overnight were normalized to an OD_{600} of 1.0, diluted 1:100 into LBS medium, and grown aerobically at 28°C. At OD_{600} = 1.0, cultures were diluted into filter-sterilized instant ocean seawater (FSSW) to 5,000 CFU/ml. Freshly hatched juveniles were exposed to

TABLE 4 Primers used in this study

Primer name	Sequence (5′→3′)
pMJM10-Ext2	CTAAAGAGGTCCCTAGCGATAAGC
170Ext	GCACTGAGAAGCCCTTAGAGCC
Deletion Alleles	
Δ*cysZ* (NPW87)	
cysZ-Del-Up-F	TAGGAACCTCTTCTCGAGCAAAAGC
cysZ-Del-Up-R	TAGGCGGCCGCACTAAGTATGGAATTTGTATTTTACTGTGTGGATGT
cysZ-Del-Down-F	GGATAGGCCTAGAAGGCCATGGTCCATAACTTATAACCTTTTGATCC
cysZ-Del-Down-R	AGCTTTAGCAATAGCTCCACCCATA
Δ*yfbS* (NPW88)	
yfbS-int-Del-Up-F	GGACTGTCACTATGGCATGGGAACA
yfbS-int-Del-Up-R	TAGGCGGCCGCACTAAGTATGGACCTAAGATAGCGGCATAAGATAAG
yfbS-int-Del-Down-F	GGATAGGCCTAGAAGGCCATGGGTGCAGCGCTTTCTATCGCACAGTT
yfbS-int-Del-Down-R	GTTTCATCCTTGAATTAAAATGGGA
Δ*cysK* (NPW90)	
cysK-Del-Up-F	ATGAATTCGTTTAAACAATCTCAAT
cysK-Del-Up-R	TAGGCGGCCGCACTAAGTATGGGATCTGTTCCTTCATTTCACGCTCA
cysK-Del-Down-F	GGATAGGCCTAGAAGGCCATGGATTTGTAACATCTATGTGTTCAAAT
cysK-Del-Down-R	AGCTTTACCTTAAAATTGATCAAAT
Promoter reporters	
PtcyJ (pVF_0008P)	
P_{tcyJ}-XmaI-u	GGCCCGGGGAAGCCAAAGCGATGAAGACACGG
P_{tcyJ}-XbaI-l	GGTCTAGAGCGAGGATATTCTTCGTCCATTTC
Overexpression vectors	
tcyP-XbaI-u	TCTAGACAAATGGGCGCATTTATGAACAGGA
tcyP-XhoI-l	CTCGAGTTAAGCTTGTGCGCTTTCTACCTGT
yfbS-XmaI-u	CCCGGGGATCTAATTAAAGAGGAGAAATTAAGCATGGCATGGGAACAAGGATTCGTTC
yfbS-SalI-l	GTCGACTTAAAATGGGAAAAAATAAGGGATT
Complement vectors	
cysK-KpnI-u1	GAGGTACCGATGTTTACCGTGATACACATAAA
cysK-SpeI-u1	GGACTAGTGGCTTGATTATTACTAAGGAGGGA

bacterial inoculums. After 3.5 hr, animals were exhaustively washed through serial transfers with FSSW to separate the squid from the *V. fischeri* cells remaining in the inoculum. Additional wash steps were performed at 24 and 48 hr post-inoculation (p.i). Immediately after washing, the bioluminescence of each animal was measured using a Glo-Max 20/20 luminometer (Promega, Madison, WI).

Abundance of *V. fischeri* within juvenile squid was determined by anesthetizing animals, homogenizing host tissue, and plating serial dilutions onto LBS medium supplemented with 1 mM cysteine. To quantify P_{tcyJ} expression within host-associated populations, animals were first anesthetized and then fixed by paraformaldehyde as previously described (Wasilko et al., 2019). Dissections were performed to reveal the light organ for microscopy. GFP, mCherry, and DIC images were acquired using a Zeiss 780 confocal microscope (Carl Zeiss AG, Jena, Germany) equipped with a 10× water lens and confocal pinholes set at a maximum for epi-fluorescence conditions. Image analysis was performed using custom scripts for ImageJ software, version 1.47 (NIH), and Matlab, version R2013a (Mathworks Inc., Natick, MA), as previously described (Wasilko et al., 2019). Briefly, mCherry fluorescence was used to identify the pixels representing *V. fischeri* populations within each image set. For each mCherry-positive pixel, the GFP/mCherry fluorescence ratio was determined and then averaged across all mCherry-positive pixels to provide a measure of P_{tcyJ} expression.

While the Pennsylvania State University does not require IACUC approval for invertebrate research, the steps described above follow recommendations for humane care and use of laboratory animals.

4.4 | Culture-based gene expression assays

Samples of cultures with strains harboring the reporter plasmid pVF0008P were harvested at the indicated time points by cooling them quickly on ice. Samples were concentrated by centrifugation

and normalized by optical density for fluorescence measurements with a Tecan fluorescent plate reader, as previously described (Wasilko et al., 2019).

4.5 | Spotting gene expression assays

Starter cultures of the indicated strains grown overnight were normalized to an OD_{600} = 1.0. A 2 μl sample was spotted onto the surface of solid medium, and the samples were incubated at 28°C. After 24 hr, the spots were examined at 4× magnification using an SZX16 fluorescence dissecting microscope (Olympus) equipped with an SDF PLFL 0.3× objective and GFP filter set. Bright field and green fluorescence images of the spot were obtained using an EOS Rebel T5 camera (Canon) with the RAW image format setting. Image analysis was performed using ImageJ (NIH) as follows. First, images were converted into RGB TIFF format using the DCRaw macro. For each spot, the green channel of the green fluorescence image was used for quantifying GFP fluorescence. First, the region of interest (ROI) corresponding to the spot was used to determine the average green fluorescence level for each spot, which is comprised of both GFP fluorescence and cellular auto-fluorescence. A non-fluorescent sample (pVSV105/ES114) was used to determine the levels of cellular auto-fluorescence. The signal associated with GFP fluorescence was then determined for calculating fold changes between groups by subtracting the auto-fluorescence levels from green fluorescence levels.

4.6 | Transposon mutagenesis screen

The reporter plasmid pVF_0008P was introduced by conjugation into the Tn*5* transposon-mutant library of ES114 that has been described elsewhere (Miyashiro et al., 2011). Recipients of the reporter plasmid were selected by plating the mating mixture onto LBS with 2.5 μg/ml chloramphenicol. The resulting colonies were screened for elevated GFP levels using an Olympus SX16 fluorescence dissecting microscope (Olympus Corp., Tokyo, Japan) equipped with a GFP filter set.

To determine the transposon insertion site within the mutant, genomic DNA was extracted from 0.5 ml LBS cultures grown overnight using the MasterPure DNA Purification Kit (Epicentre Biotechnologies, Madison, WI). Approximately 10 μg genomic DNA was digested by EcoRI-HF (New England Biolabs, Ipswich, MA) in a 40 μl reaction at 37°C. After 3 hr at 37°C, the enzyme was removed using an Omega E.Z.N.A. Cycle Pure Kit. The DNA was self-ligated using T4 DNA ligase (New England Biolabs) and electroporated into S17-1λpir and selected on BHI +150 μg/ml erythromycin. Plasmid DNA was extracted using an Omega E.Z.N.A. plasmid minikit and sequenced at the Penn State Nucleic Acid Facility (Pennsylvania State University) with transposon-specific primers pMJM10-Ext2 and 170Ext.

4.7 | Seawater abundance assay

Starter cultures grown overnight were diluted 1:100 into LBS and incubated aerobically with shaking at 28°C. After 2 hr, cells were normalized to OD_{600} = 1.0, and a 1 ml sample was centrifuged at 15,000×*g*. After 2 min, the supernatant was removed, and the pellets were washed twice with 1 ml FSSW. Wash step was repeated one additional time. Samples were diluted 1:100 by introducing 20 μl of the cell suspension into 14 ml polystyrene tubes containing 2 ml FSSW and incubated at room temperature in a roller drum. Samples were serially diluted at the indicated time points and plated onto LBS medium supplemented with cysteine, as described elsewhere (Wasilko et al., 2019). The corresponding CFU counts were used to calculate strain abundance.

4.8 | Bioinformatics analyses

4.8.1 | Prediction of domains in YfbS

Transmembrane domains were predicted by TMHMM server 2.0 (Moller et al., 2001) using as query NCBI RefSeq WP_011261126.1. The two TrkA_C domains are based on homology with pfam02080.

4.8.2 | Identification of CysC and YfbS homologs

Representative species were identified for each of the 23 major clades of *Vibrionaceae* previously reported (Sawabe et al., 2013). Their genomes were identified at ncbi.nlm.nih.gov and subject to two searches using BLAST-based tools. Each search used the tBLASTn algorithm with the queries as: (1) the *V. fischeri* CysC homolog (Accession: NC_006840.2; locus_tag: VF_0323) and (2) the *V. fischeri* YfbS homolog (Accession: NC_006840.2; locus_tag: VF_0322). For the species for which tBLASTn searches failed, genome assembly and annotation reports for those species (www.ncbi.nlm.nih.gov/genome) were searched for contigs/scaffolds with matching sequences. Results from searches performed from June 2020 through July 2020 have been reported in Table S1.

4.8.3 | Phylogenetic tree construction

A supertree illustrating the phylogenetic relationship among *Vibrionaceae* members was previously reported (Sawabe et al., 2013). To highlight the relatedness of taxa examined in this study, the supertree was superimposed over a grid-lined workspace with Inkscape 0.92, and the branch corresponding to each taxon was copied, with branch lengths and nodal arrangements/spacing preserved. Taxa present in Table S1 were connected into clades using the most derived node present in the original supertree (Sawabe et al., 2013). For each species present in the supertree but not included in Table S1,

the taxon and its associated branch were removed from the tree. A png file was exported from Inkscape, flattened, and scaled in GIMP 2.10.08 to create Figure 6a.

4.8.4 | [^{35}S]-sulfate uptake assay

Starter cultures of the indicated strains were initiated by inoculating 3 ml LBS supplemented with 1 mM cysteine with an isolated colony and incubated at 28°C by shaking (200 rpm). After approximately 20 hr, starter cultures were normalized to an OD_{600} = 1.0, and 30 µl of the cell suspension was used to inoculate 3 ml defined minimal medium supplemented with 18.5 µM cystine and 0.1 mM sulfate. Cultures were incubated at 28°C with shaking. When cultures achieved OD_{600} ~0.8, cells were concentrated to an effective OD_{600} of 3.75 by centrifugation at 9,000×*g* for 2 min and resuspending in 0.5 ml of fresh medium and held at 28°C. Reactions were initiated by combining 0.4 ml of a cell suspension with 1.1 ml of a [^{35}S] sulfate cocktail in cystine/sulfate defined minimal medium, with sulfate at a final concentration of 0.1 mM and 167 mCi/mmol. [^{35}S] sulfate was purchased from PerkinElmer. At each time point, a 0.2 ml sample was applied to a prewashed 25 mm Grade GF/F Whatman Glass microfiber filter, which was washed three times with sulfate-free defined minimal medium using a 1,225 vacuum manifold (Millipore) and placed into a scintillation vial. After all time points have passed, 5 ml of scintillation fluid (ScintiSafe Econo F) was added, and the counts recorded over a 1-min interval were measured in a Beckman Coulter LS 6,500 Multi-Purpose Scintillation Counter.

4.9 | Statistical analyses

Statistical analyses were performed using Prism v. 8.4.3 software (Graphpad, La Jolla, CA, USA).

ACKNOWLEDGEMENTS

This work was supported by National Institutes of Health grant R01 GM129133 (to TIM) and the Penn State University/NIDDK-funded Integrative Analysis of Metabolic Phenotypes (IAMP) pre-doctoral training program T32 DK120509 (to JSC). We thank members of the Miyashiro lab for constructive criticism of this project. We also thank Dr. Emily Weinert for the *E. coli* mutants from the Keio collection and Drs. Kenneth C. Keiler and John N. Alumasa for their assistance in conducting the sulfate-uptake assays. We also thank the three anonymous reviewers and the editor for their feedback on our manuscript.

CONFLICT OF INTEREST

The authors declare no conflict of interest.

AUTHOR CONTRIBUTIONS

Except for the contributions listed below, NPW and TIM contributed to all aspects of the study, including experimental design; acquisition, analysis, and interpretation of data; and writing the manuscript. JSC contributed to the culture-based gene expression assays and *E. coli* culture growth experiments. ERB contributed to the squid colonization assays and culture growth assays. AGC contributed to constructing the *cysK* complementation vector and performing the spotting gene expression and sulfate uptake assays. MSW and TIM conducted the bioinformatics study of YfbS and CysC homologs in *Vibrionaceae*.

DATA AVAILABILITY STATEMENT

The data that support the findings of this study are available from the corresponding author upon reasonable request.

ORCID

Tim I. Miyashiro https://orcid.org/0000-0002-5016-1641

REFERENCES

Aguilar-Barajas, E., Diaz-Perez, C., Ramirez-Diaz, M.I., Riveros-Rosas, H. & Cervantes, C. (2011) Bacterial transport of sulfate, molybdate, and related oxyanions. *BioMetals*, *24*(4), 687–707. https://doi.org/10.1007/s10534-011-9421-x

Amann, E., Ochs, B. & Abel, K.J. (1988) Tightly regulated *tac* promoter vectors useful for the expression of unfused and fused proteins in *Escherichia coli*. *Gene*, *69*(2), 301–315. https://doi.org/10.1016/0378-1119(88)90440-4

Anderson, M.T., Mitchell, L.A., Sintsova, A., Rice, K.A. & Mobley, H.L.T. (2019) Sulfur assimilation alters flagellar function and modulates the gene expression landscape of *Serratia marcescens*. *mSystems*, *4*(4), e00285-19. https://doi.org/10.1128/mSystems.00285-19

Assur Sanghai, Z., Liu, Q., Clarke, O.B., Belcher-Dufrisne, M., Wiriyasermkul, P., Giese, M.H. et al. (2018) Structure-based analysis of CysZ-mediated cellular uptake of sulfate. *Elife*, *7*, e27829. https://doi.org/10.7554/eLife.27829

Baba, T., Ara, T., Hasegawa, M., Takai, Y., Okumura, Y., Baba, M. et al. (2006) Construction of *Escherichia coli* K-12 in-frame, single-gene knockout mutants: the Keio collection. *Molecular Systems Biology*, *2*, 2006 0008. https://doi.org/10.1038/msb4100050

Bao, Y., Lies, D.P., Fu, H. & Roberts, G.P. (1991) An improved Tn7-based system for the single-copy insertion of cloned genes into chromosomes of gram-negative bacteria. *Gene*, *109*(1), 167–168. https://doi.org/10.1016/0378-1119(91)90604-A

Bose, J.L., Rosenberg, C.S. & Stabb, E.V. (2008) Effects of *luxCDABEG* induction in *Vibrio fischeri*: enhancement of symbiotic colonization and conditional attenuation of growth in culture. *Archives of Microbiology*, *190*(2), 169–183. https://doi.org/10.1007/s00203-008-0387-1

Chonoles Imlay, K.R., Korshunov, S. & Imlay, J.A. (2015) Physiological roles and adverse effects of the two cystine importers of *Escherichia coli*. *Journal of Bacteriology*, *197*(23), 3629–3644. https://doi.org/10.1128/JB.00277-15

Crane, B.R. & Getzoff, E.D. (1996) The relationship between structure and function for the sulfite reductases. *Current Opinion in Structural Biology*, *6*(6), 744–756. https://doi.org/10.1016/s0959-440x(96)80003-0

Datsenko, K.A. & Wanner, B.L. (2000) One-step inactivation of chromosomal genes in *Escherichia coli* K-12 using PCR products. *Proceedings of the National Academy of Sciences USA*, *97*(12), 6640–6645. https://doi.org/10.1073/pnas.120163297

Dreyfuss, J. (1964) Characterization of a sulfate- and thiosulfate-transporting system in *Salmonella typhimurium*. *Journal of Biological Chemistry*, *239*, 2292–2297. https://doi.org/10.1016/S0021-9258(20)82233-9

Dunn, A.K., Millikan, D.S., Adin, D.M., Bose, J.L. & Stabb, E.V. (2006) New *rfp*- and pES213-derived tools for analyzing symbiotic *Vibrio fischeri* reveal patterns of infection and *lux* expression in situ. *Applied and Environment Microbiology*, *72*(1), 802–810. https://doi.org/10.1128/AEM.72.1.802-810.2006

Gisin, J., Muller, A., Pfander, Y., Leimkuhler, S., Narberhaus, F. & Masepohl, B. (2010) A *Rhodobacter capsulatus* member of a universal permease family imports molybdate and other oxyanions. *Journal of Bacteriology*, *192*(22), 5943–5952. https://doi.org/10.1128/JB.00742-10

Graf, J. & Ruby, E.G. (1998) Host-derived amino acids support the proliferation of symbiotic bacteria. *Proceedings of the National Academy of Sciences USA*, *95*(4), 1818–1822. https://doi.org/10.1073/pnas.95.4.1818

Guckes, K.R., Cecere, A.G., Williams, A.L., Mcneil, A.E. & Miyashiro, T. (2020) The bacterial enhancer binding protein VasH promotes expression of a Type VI secretion system in *Vibrio fischeri* during symbiosis. *Journal of Bacteriology*, *202*(7), e00777-19. https://doi.org/10.1128/JB.00777-19

Hoffmann, M.C., Pfander, Y., Tintel, M. & Masepohl, B. (2017) Bacterial PerO permeases transport sulfate and related oxyanions. *Journal of Bacteriology*, *199*(14), e00183-17. https://doi.org/10.1128/JB.00183-17

Hulanicka, M.D., Kredich, N.M. & Treiman, D.M. (1974) The structural gene for *O*-acetylserine sulfhydrylase A in *Salmonella typhimurium*. Identity with the *trzA* locus. *Journal of Biological Chemistry*, *249*(3), 867–872.

Jones, B.W. & Nishiguchi, M.K. (2004) Counterillumination in the Hawaiian bobtail squid, *Euprymna scolopes* Berry (Mollusca: Cephalopoda). *Marine Biology*, *144*, 1151–1155. https://doi.org/10.1007/s00227-003-1285-3

Kredich, N.M. (1992) The molecular basis for positive regulation of *cys* promoters in *Salmonella typhimurium* and *Escherichia coli*. *Molecular Microbiology*, *6*(19), 2747–2753.

Kredich, N.M. (2008) Biosynthesis of cysteine. *EcoSal Plus*, *3*(1). https://doi.org/10.1128/ecosalplus.3.6.1.11

Kredich, N.M. & Tomkins, G.M. (1966) The enzymic synthesis of L-cysteine in *Escherichia coli* and *Salmonella typhimurium*. *Journal of Biological Chemistry*, *241*(21), 4955–4965. https://doi.org/10.1016/S0021-9258(18)99657-2

Kutsche, M., Leimkuhler, S., Angermuller, S. & Klipp, W. (1996) Promoters controlling expression of the alternative nitrogenase and the molybdenum uptake system in *Rhodobacter capsulatus* are activated by NtrC, independent of sigma54, and repressed by molybdenum. *Journal of Bacteriology*, *178*(7), 2010–2017. https://doi.org/10.1128/jb.178.7.2010-2017.1996

Lee, K.H. & Ruby, E.G. (1994) Effect of the squid host on the abundance and distribution of symbiotic *Vibrio fischeri* in nature. *Applied and Environment Microbiology*, *60*(5), 1565–1571.

Lensmire, J.M., Dodson, J.P., Hsueh, B.Y., Wischer, M.R., Delekta, P.C., Shook, J.C. et al. (2020) The *Staphylococcus aureus* cystine transporters TcyABC and TcyP facilitate nutrient sulfur acquisition during infection. *Infection and Immunity*, *88*(3), e00690-19. https://doi.org/10.1128/IAI.00690-19

Lensmire, J.M. & Hammer, N.D. (2018) Nutrient sulfur acquisition strategies employed by bacterial pathogens. *Current Opinion in Microbiology*, *47*, 52–58. https://doi.org/10.1016/j.mib.2018.11.002

Mccann, J., Stabb, E.V., Millikan, D.S. & Ruby, E.G. (2003) Population dynamics of *Vibrio fischeri* during infection of *Euprymna scolopes*. *Applied and Environment Microbiology*, *69*(10), 5928–5934.

Miller, J.H. (1972) *Experiments in molecular genetics*. Cold Spring Harbor Laboratory.

Millero, F.J. (2014) *Physico-chemical controls on seawater*. Elsevier.

Miyashiro, T., Klein, W., Oehlert, D., Cao, X., Schwartzman, J. & Ruby, E.G. (2011) The N-acetyl-D-glucosamine repressor NagC of *Vibrio fischeri* facilitates colonization of *Euprymna scolopes*. *Molecular Microbiology*, *82*(4), 894–903. https://doi.org/10.1111/j.1365-2958.2011.07858.x

Miyashiro, T., Wollenberg, M.S., Cao, X., Oehlert, D. & Ruby, E.G. (2010) A single *qrr* gene is necessary and sufficient for LuxO-mediated regulation in *Vibrio fischeri*. *Molecular Microbiology*, *77*(6), 1556–1567. https://doi.org/10.1111/j.1365-2958.2010.07309.x

Moller, S., Croning, M.D. & Apweiler, R. (2001) Evaluation of methods for the prediction of membrane spanning regions. *Bioinformatics*, *17*(7), 646–653. https://doi.org/10.1093/bioinformatics/17.7.646

Montgomery, M.K. & Mcfall-Ngai, M. (1993) Embryonic development of the light organ of the sepiolid squid *Euprymna scolopes* Berry. *Biological Bulletin (Woods Hole)*, *184*(3), 296–308. https://doi.org/10.2307/1542448

Pajor, A.M. (2006) Molecular properties of the SLC13 family of dicarboxylate and sulfate transporters. *Pflugers Archiv. European Journal of Physiology*, *451*(5), 597–605. https://doi.org/10.1007/s00424-005-1487-2

Pardee, A.B. (1966) Purification and properties of a sulfate-binding protein from *Salmonella typhimurium*. *Journal of Biological Chemistry*, *241*(24), 5886–5892.

Parra, F., Britton, P., Castle, C., Jones-Mortimer, M.C. & Kornberg, H.L. (1983) Two separate genes involved in sulphate transport in *Escherichia coli* K12. *Journal of General Microbiology*, *129*(2), 357–358. https://doi.org/10.1099/00221287-129-2-357

Psychogios, N., Hau, D.D., Peng, J., Guo, A.C., Mandal, R., Bouatra, S. et al. (2011) The human serum metabolome. *PLoS One*, *6*(2), e16957. https://doi.org/10.1371/journal.pone.0016957

Ruby, E.G., Urbanowski, M., Campbell, J., Dunn, A., Faini, M., Gunsalus, R. et al. (2005) Complete genome sequence of *Vibrio fischeri*: a symbiotic bacterium with pathogenic congeners. *Proceedings of the National Academy of Sciences USA*, *102*(8), 3004–3009. https://doi.org/10.1073/pnas.0409900102

Sawabe, T., Ogura, Y., Matsumura, Y., Feng, G., Amin, A.R., Mino, S. et al. (2013) Updating the Vibrio clades defined by multilocus sequence phylogeny: proposal of eight new clades, and the description of *Vibrio tritonius* sp. nov. *Frontiers in Microbiology*, *4*, 414. https://doi.org/10.3389/fmicb.2013.00414

Schwartzman, J.A., Koch, E., Heath-Heckman, E.A., Zhou, L., Kremer, N., Mcfall-Ngai, M.J. et al. (2015) The chemistry of negotiation: rhythmic, glycan-driven acidification in a symbiotic conversation. *Proceedings of the National Academy of Sciences USA*, *112*(2), 566–571. https://doi.org/10.1073/pnas.1418580112

Siegel, L.M., Rueger, D.C., Barber, M.J., Krueger, R.J., Orme-Johnson, N.R. & Orme-Johnson, W.H. (1982) *Escherichia coli* sulfite reductase hemoprotein subunit. Prosthetic groups, catalytic parameters, and ligand complexes. *Journal of Biological Chemistry*, *257*(11), 6343–6350.

Singh, P., Brooks, J.F. 2nd, Ray, V.A., Mandel, M.J. & Visick, K.L. (2015) CysK plays a role in biofilm formation and colonization by *Vibrio fischeri*. *Applied and Environment Microbiology*, *81*(15), 5223–5234. https://doi.org/10.1128/AEM.00157-15

Sirko, A., Zatyka, M., Sadowy, E. & Hulanicka, D. (1995) Sulfate and thiosulfate transport in *Escherichia coli* K-12: evidence for a functional overlapping of sulfate- and thiosulfate-binding proteins. *Journal of Bacteriology*, *177*(14), 4134–4136. https://doi.org/10.1128/jb.177.14.4134-4136.1995

Soutourina, O., Poupel, O., Coppee, J.Y., Danchin, A., Msadek, T. & Martin-Verstraete, I. (2009) CymR, the master regulator of cysteine metabolism in *Staphylococcus aureus*, controls host sulphur source utilization and plays a role in biofilm formation. *Molecular Microbiology*, *73*(2), 194–211. https://doi.org/10.1111/j.1365-2958.2009.06760.x

Stabb, E.V. & Ruby, E.G. (2002) RP4-based plasmids for conjugation between *Escherichia coli* and members of the *Vibrionaceae*. *Methods in Enzymology*, *358*, 413–426.

Stabb, E.V. & Visick, K.L. (2013) *Vibrio fischeri*: a bioluminescent light-organ symbiont of the bobtail squid euprymna scolopes. In: Rosenberg, E., Delong, E.F., Stackebrand, E., Lory, S. & Thompson, F. (Eds.) *The prokaryotes – prokaryotic biology and symbiotic associations*. Springer-Verlag, pp. 497–532.

Visick, K.L., Hodge-Hanson, K.M., Tischler, A.H., Bennett, A.K. & Mastrodomenico, V. (2018) Tools for rapid genetic engineering of *Vibrio fischeri*. *Applied and Environment Microbiology*, *84*(14), e00850-18. https://doi.org/10.1128/AEM.00850-18

Wasilko, N.P., Larios-Valencia, J., Steingard, C.H., Nunez, B.M., Verma, S.C. & Miyashiro, T. (2019) Sulfur availability for *Vibrio fischeri* growth during symbiosis establishment depends on biogeography within the squid light organ. *Molecular Microbiology*, *111*(3), 621–636. https://doi.org/10.1111/mmi.14177

Wier, A.M., Nyholm, S.V., Mandel, M.J., Massengo-Tiasse, R.P., Schaefer, A.L., Koroleva, I. et al. (2010) Transcriptional patterns in both host and bacterium underlie a daily rhythm of anatomical and metabolic change in a beneficial symbiosis. *Proceedings of the National Academy of Sciences USA*, *107*(5), 2259–2264. https://doi.org/10.1073/pnas.0909712107

Wishart, D.S., Feunang, Y.D., Marcu, A., Guo, A.C., Liang, K., Vazquez-Fresno, R. et al. (2018) HMDB 4.0: the human metabolome database for 2018. *Nucleic Acids Research*, *46*(D1), D608–D617. https://doi.org/10.1093/nar/gkx1089

Zink, K.E., Tarnowski, D.A., Mandel, M.J. & Sanchez, L.M. (2020) Optimization of a minimal sample preparation protocol for imaging mass spectrometry of unsectioned juvenile invertebrates. *Journal of Mass Spectrometry*, *55*(4), e4458. https://doi.org/10.1002/jms.4458

SUPPORTING INFORMATION

Additional Supporting Information may be found online in the Supporting Information section.

How to cite this article: Wasilko, N.P., Ceron, J.S., Baker, E.R., Cecere, A.G., Wollenberg, M.S. & Miyashiro, T.I. (2021) *Vibrio fischeri* imports and assimilates sulfate during symbiosis with *Euprymna scolopes*. *Molecular Microbiology*, 116, 926–942. https://doi.org/10.1111/mmi.14780